

Effect of purification pretreatment on the recovery of magnetite from waste ferrous sulfate

Wang Yu¹⁾, Ying-lin Peng²⁾, and Ya-jie Zheng¹⁾

1) School of Metallurgy and Environment, Central South University, Changsha 410083, China

2) School of Chemistry and Environmental Engineering, Hunan City University, Yiyang 413000, China

(Received: 7 January 2016; revised: 18 April 2016; accepted: 21 April 2016)

Abstract: The present study was conducted to elucidate the influence of impurities in waste ferrous sulfate on its recovery of magnetite. Ferrous sulfate solution was purified by the addition of NaOH solution to precipitate impurities, and magnetite was recovered from ferrous sulfate solution without and with purification pretreatment. Calcium hydroxide was added to the solution of ferrous sulfate as a precipitator. A mixed product of magnetite and gypsum was subsequently obtained by air oxidation and heating. Wet-milling was performed prior to magnetic separation to recover magnetite from the mixed products. The results show that with the purification pretreatment, the grade of iron in magnetite concentrate increased from 62.05% to 65.58% and the recovery rate of iron decreased from 85.35% to 80.35%. The purification pretreatment reduced the conglutination between magnetite and gypsum, which favors their subsequent magnetic separation. In summary, a higher-grade magnetite with a better crystallinity and a larger particle size of 2.35 μm was obtained with the purification pretreatment.

Keywords: ferrous sulfate; titanium dioxide; purification; magnetite; magnetic separation

1. Introduction

Ferrous sulfate is a major industrial byproduct of titanium dioxide manufacture via the sulfate method, and its main mineral component is $\text{FeSO}_4 \cdot 7\text{H}_2\text{O}$. By the end of 2013, the total ferrous sulfate production in China was greater than 7×10^6 t, and the annual growth rate of production exceeded 10% [1]. Unfortunately, this waste is less marketable and is difficult to utilize because of its high impurity content [2], which causes not only severe environmental problems but also the waste of iron resources. As a consequence, an urgent need exists to utilize this solid waste in an effective manner.

Many methods have been used to treat ferrous sulfate, which can be used to manufacture iron oxides, water-treatment coagulants, alkali ferrates, cation-substituted LiFePO_4 , and iron(III) tanning salts, among other compounds [3–9]. To our knowledge, using of $\text{FeSO}_4 \cdot 7\text{H}_2\text{O}$ to produce iron oxides could be one of the most effective

methods for waste reduction [3]. Magnetic particles (Fe_3O_4) are currently being widely studied in the wastewater flocculation field [10–12]. In this context, our aim in the present study is to use $\text{FeSO}_4 \cdot 7\text{H}_2\text{O}$ to recover Fe_3O_4 particles for magnetic seeding flocculation in water and wastewater treatment. However, various impurities in the waste ferrous sulfate adversely affect the properties of the resultant iron oxides [8], and research into the effect of impurities in waste ferrous sulfate on its suitability as a precursor for the preparation of iron oxides is scarce.

The present study is conducted to elucidate the influence of impurities in waste ferrous sulfate on its recovery of Fe_3O_4 . Purification pretreatment was performed by adding NaOH solution to ferrous sulfate solution to precipitate impurities. Subsequently, magnetite was recovered from ferrous sulfate solution without and with purification pretreatment. The effect of purification pretreatment prior to the magnetite recovery on the grade of iron in magnetite concentrate was analyzed.

Corresponding author: Ya-jie Zheng E-mail: zyj@csu.edu.cn

© University of Science and Technology Beijing and Springer-Verlag Berlin Heidelberg 2016

2. Experimental

2.1. Materials

Reagent-grade NaOH and CaO (Guangdong Xilong Chemical Co., Ltd.) were used without further purification. Dried ferrous sulfate was provided by Guangdong Huiyun Titanium Industry Co. Ltd., China. The dried ferrous sulfate sample was further dried in a vacuum atmosphere at 80°C for 12 h, and its chemical composition was subsequently analyzed by X-ray fluorescence (XRF); the results are shown in Table 1. The sample was composed of O (39.24wt%), Fe (36.08wt%), S (22.11wt%), and various impurity elements.

Table 1. Chemical composition of dried ferrous sulfate wt%

O	Fe	S	Mg	Ti	Mn	Zn	Al
39.24	36.08	22.11	1.24	0.89	0.31	0.02	0.02

2.2. Purification pretreatment

The purification experiments were carried out by adding NaOH solution to ferrous sulfate solution to precipitate impurities. The effect of pH value on impurity removal was investigated in the pH range from 2.5 to 5.0. 400 mL of ferrous sulfate solution with an Fe^{2+} ion concentration of 1 mol/L was added to a 500 mL beaker on a magnetic stirrer. The solution pH value was adjusted to a certain range by dropwise addition of NaOH solution of different concentrations, followed by continuous stirring for 30 min at room temperature. The solution was finally filtered under vacuum, and the filtrate was analyzed for volume and chemical composition. All the experiments were conducted in duplicate; the average values are presented.

2.3. Magnetite recovery

On the basis of the previously described purification experiments, magnetite was recovered from ferrous sulfate solutions without and with purification at the optimum pH value of 3.5–4.0. Magnetite was recovered using the following procedure: 4 L of ferrous sulfate solution with an Fe^{2+} ion concentration of 0.4 mol/L was added to a 5-L, four-necked flask fitted with a reflux condenser and electric heater. To obtain lime milk, we added purified water to calcium oxide (CaO) at a liquid to solid mass ratio of 3:1 under vigorous stirring. The lime milk with a 1.4:1 molar ratio of $\text{CaO}/\text{Fe}^{2+}$ was added dropwise to the solution under sufficient stirring. The reactor was heated to 80°C, and air was bubbled into the solution at 0.6 m³/h. When the molar ratio of $\text{Fe}^{3+}/\text{Fe}^{2+}$ in the reaction solution reached 1.9–2.1, the re-

action was stopped. The obtained mixture of magnetite and gypsum was then filtrated, dried, and ground for use in subsequent experiments.

The wet-milling pretreatment was conducted at room temperature in a ball mill using a slurry with a mixed product-to-water mass ratio of 1:40 and a rotation speed of 130 r/min. The time of milling was 20 min, and the treated mixed product was directly subjected to magnetic separation. Magnetic separation was performed using a low-intensity magnetic separator (CRIMM DC CXGφ50, Changsha Research Institute of Mining and Metallurgy Co., Ltd., China), with a working electrical current of 1.75 A (a magnetic field intensity of 1750 Gs). The magnetic fractions were washed, filtered, weighed, and subjected to various analyses.

The whole procedure used to recover magnetite from ferrous sulfate is summarized in Fig. 1.

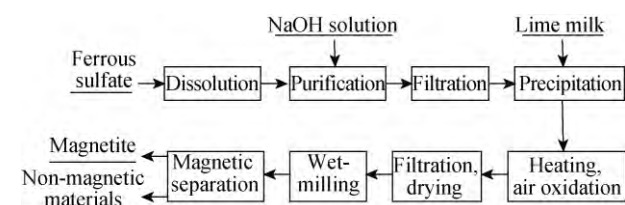


Fig. 1. Flow sheet of magnetite recovery from ferrous sulfate.

2.4. Analysis

The samples were analyzed according to Chinese Standard GB/T 1863—2008 to examine their ferrous and ferric ion content [13]. The content of impurity elements in the solution was determined by inductively coupled plasma optical emission spectrometry (ICP-OES, iCAP 7000 Series, Thermo Scientific). Phase analysis of the samples was conducted on a Rigaku D/max-TTR III X-ray diffractometer (XRD) equipped with a Cu K_{α} radiation source ($\lambda = 0.154056$ nm) operated at a voltage of 40 kV, a current of 250 mA, and a scanning rate of 10°/min from 10° to 70°. The raw material sample was measured by XRF with a Bruker S4 Pioneer system equipped with two X-ray detectors. The surface morphology of the samples was observed using an FEI Quanta 200 scanning electron microscope (SEM) coupled with an energy dispersive X-ray spectroscope (EDS). A laser particle size analyzer (LS-pop (6), Zhuhai OMEC Instrument Co., Ltd.) was used to analyze the size distribution of the samples.

3. Results and discussion

3.1. Purification pretreatment

According to the titration and ICP-OES analysis results,

the initial solution obtained after dissolution of ferrous sulfate had a composition of Fe(II) 56.000 g/L, total Fe 57.898 g/L, Mg 1.754 g/L, Ti 1.703 g/L, Mn 0.788 g/L, Zn 0.178 g/L, and Al 0.153 g/L, which is in agreement with the XRF results (Table 1). In this study, the initial ferrous sulfate solution with a pH value of 1.7–1.9 was purified by the addition of NaOH solution; the experimental results are shown in Table 2. The results in Table 2 demonstrate that the concentrations of Fe(II), total Fe, Ti, Zn, and Al in purified ferrous sulfate solutions were gradually decreased with increasing pH value; Ti, in particular, was almost completely precipitated at pH levels greater than 3.5. No significant changes in the concentrations of Mg and Mn were observed in the investigated pH range, suggesting no or very little precipitation of these two elements.

Table 2. Volumes and compositions of ferrous sulfate solutions purified under different pH conditions

pH	Volume / mL	Composition / (g·L ⁻¹)						
		Fe(II)	Total Fe	Mg	Ti	Mn	Zn	Al
2.5–3.0	392	55.888	57.344	1.757	1.367	0.793	0.178	0.146
3.0–3.5	391	55.888	56.896	1.748	1.231	0.795	0.154	0.099
3.5–4.0	391	52.808	52.808	1.755	0.028	0.795	0.142	0.074
4.0–4.5	391	52.438	52.438	1.744	0.002	0.788	0.104	0.045
4.5–5.0	390	51.856	51.856	1.739	0.002	0.788	0.094	0.029

The removal rates of metals as a function of pH value are shown in Fig. 2. At pH levels greater than 3.5, according to the removal rates, the metal precipitation order was Ti > Al > Zn > Fe. For example, at pH 3.5–4.0, the removal rates of Ti, Al, Zn, and Fe were 98.39%, 52.72%, 22.02%, and 10.84%, respectively. However, an increase in pH value did not substantially affect the precipitation of Mg and Mn, as indicated by the lack of substantial change in their removal rates. At pH 3.5–4.0, the removal rates of Mg and Mn were only 2.19% and 1.38%, respectively.

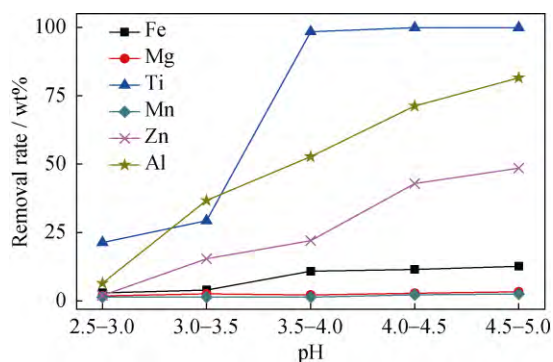


Fig. 2. Removal rates of metals in purified ferrous sulfate solutions under different pH conditions.

Precipitating impurities as their respective hydroxides by raising the pH value of the solution is a commonly used technique in hydrometallurgical processing [14]. Whether a metal ion M^{n+} in a certain concentration will form an insoluble hydroxide precipitate depends on the concentration of OH^- ions in the solution, i.e., the pH of the solution is the most important parameter governing the precipitation of metal hydroxides. If M^{n+} and OH^- generate only $M(OH)_n$ precipitates without generating soluble hydroxy complexes, the pH value at which hydroxides begin to precipitate can be calculated in accordance with the solubility product constant (K_{sp}) of the metal hydroxides and the ionic product constant (pK_w) of water as follows:

$$\lg C(M^{n+}) = \lg K_{sp} + npK_w - npH \quad (1)$$

where $C(M^{n+})$ is the concentration of M^{n+} , mol/L. According to Eq. (1), under certain conditions of temperature and metal ion concentration, the pH value increases with increasing K_{sp} . The reference K_{sp} values of relevant metal hydroxides [15] at 18–25°C are listed in Table 3. We inferred from the results in Table 3 that the metal precipitation order with increasing pH value is $Ti(OH)_3 > Fe(OH)_3 > Al(OH)_3 > TiO(OH)_2 > Zn(OH)_2 > Fe(OH)_2 > Mn(OH)_2 > Mg(OH)_2$, which is consistent with the results in Fig. 2. With respect to precipitating some impurities and minimizing iron loss, the optimum pH value is 3.5–4.0.

Table 3. Reference K_{sp} values of relevant metal hydroxides at 18–25°C

Metal hydroxide	K_{sp}	Metal hydroxide	K_{sp}
$Ti(OH)_3$	1.00×10^{-40}	$Zn(OH)_2$	3.00×10^{-17}
$Fe(OH)_3$	2.49×10^{-39}	$Fe(OH)_2$	4.87×10^{-17}
$Al(OH)_3$	1.30×10^{-33}	$Mn(OH)_2$	1.90×10^{-13}
$TiO(OH)_2$	1.00×10^{-29}	$Mg(OH)_2$	5.61×10^{-12}

3.2. Magnetite recovery

3.2.1. Effect of purification pretreatment on the preparation of a mixed product

In this study, the mixed product of magnetite and gypsum can be formed from ferrous sulfate solution with calcium hydroxide as the precipitant according to the following reactions [16]:

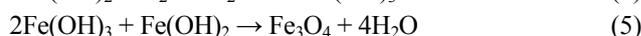
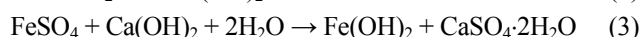


Fig. 3 shows XRD patterns of the mixed products without and with purification pretreatment. The patterns of the two mixed products both possessed the peaks characteristic

of Fe_3O_4 (JCPDS No. 19-0629) and $\text{CaSO}_4 \cdot 2\text{H}_2\text{O}$ (JCPDS No. 33-0311). In addition, the peaks of both Fe_3O_4 and $\text{CaSO}_4 \cdot 2\text{H}_2\text{O}$ became sharper and narrower with purification pretreatment, which indicates that the obtained particles exhibited higher crystallinity and a larger particle size. The X-ray diffraction peaks reflect the degree of crystallinity and the size of the particles. More intense diffraction peaks indicate more extensive crystallization of particles, and the half-peak width decreases with increasing particle size [17]. The particle size distribution of the mixed products without and with purification pretreatment is shown in Fig. 4. From Fig. 4, it is evident that the particle size of the mixed product obtained with pretreatment was bigger than that of the product without pretreatment, and their median particle sizes were 2.31 and 2.05 μm , respectively. This finding is consistent with the aforementioned XRD results.

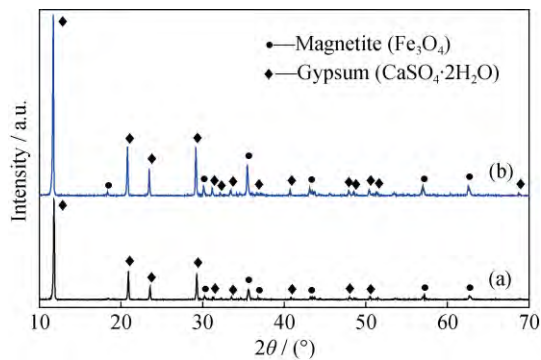


Fig. 3. XRD patterns of the mixed products without (a) and with (b) purification pretreatment.

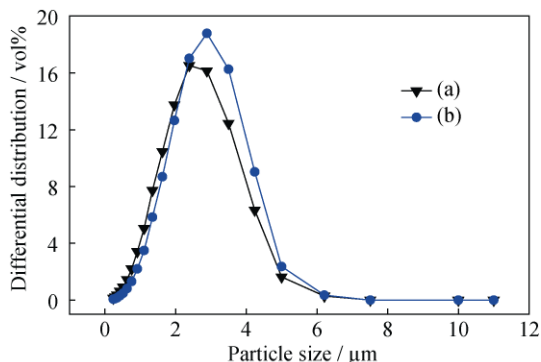


Fig. 4. Particle size distribution of the mixed products without (a) and with (b) purification pretreatment.

Figs. 5(a) and 5(b) display SEM images of the mixed products. The corresponding EDS spectra are also presented in Fig. 5(c)–5(f). In Figs. 5(a) and 5(b), two distinct phases were observed: A and C were irregularly shaped plates, whereas fine B and D were apt to aggregate. Subsequent EDS analysis demonstrated that the two phases were gyp-

sum (A and C) and magnetite (B and D), in agreement with the XRD results in Fig. 3. Moreover, comparing the EDS spectra of A and C reveals that the Fe content in the C phase (gypsum) was lower than that in the A phase and that the Ca and S contents in the D phase (magnetite) were lower than those in the B phase. We inferred that the purification pretreatment can reduce the conglutination between magnetite and gypsum, which favors their subsequent magnetic separation.

3.2.2. Effect of purification pretreatment on the recovery of magnetite

Magnetite was recovered from the mixed product by magnetic separation. The original grades of iron in the mixed product without and with purification pretreatment were determined by titration to be 20.16% and 20.55%, respectively. With purification pretreatment, the grade of iron in the magnetite concentrate increased from 62.05% to 65.58%, whereas the recovery rate of iron decreased from 85.35% to 80.35%. This finding is compatible with the SEM analysis results in Fig. 5. Fig. 6 shows the XRD patterns of magnetite concentrates obtained without and with purification pretreatment. These XRD patterns of the two concentrates both included eight obvious diffraction peaks representing corresponding indices (111), (220), (311), (222), (400), (422), (511), and (440) of magnetite. The position and relative intensity of all of these diffraction peaks matched well with the reflections of the standard Fe_3O_4 . However, the diffraction peak intensity of Fe_3O_4 was enhanced with purification pretreatment, indicating that the obtained products contained more Fe_3O_4 phase with a better degree of crystallization [18]. These results agree well with the aforementioned titration results. However, a peak attributable to CaCO_3 emerged in the patterns of both of the products. The reaction to form calcite can be expressed by the following reaction:

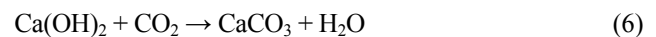


Fig. 7 displays SEM images of magnetite concentrates. As shown in Fig. 7, spherical-shaped Fe_3O_4 particles were observed in both concentrates; however, Fe_3O_4 particles were apt to aggregate because of their large specific surface area (surface-to-volume ratio) and high surface energy [19–20]. In addition, the particle size of the concentrate obtained with purification pretreatment increased. Fe_3O_4 has been proposed to be formed by air-oxidation of $\text{Fe}(\text{OH})_2$ via dissolution and recrystallization [21]. The particle size is related to the nucleation and growth rate of the primary particles [22], which may depend on the content of impurities in the reaction solution. In the absence of purification

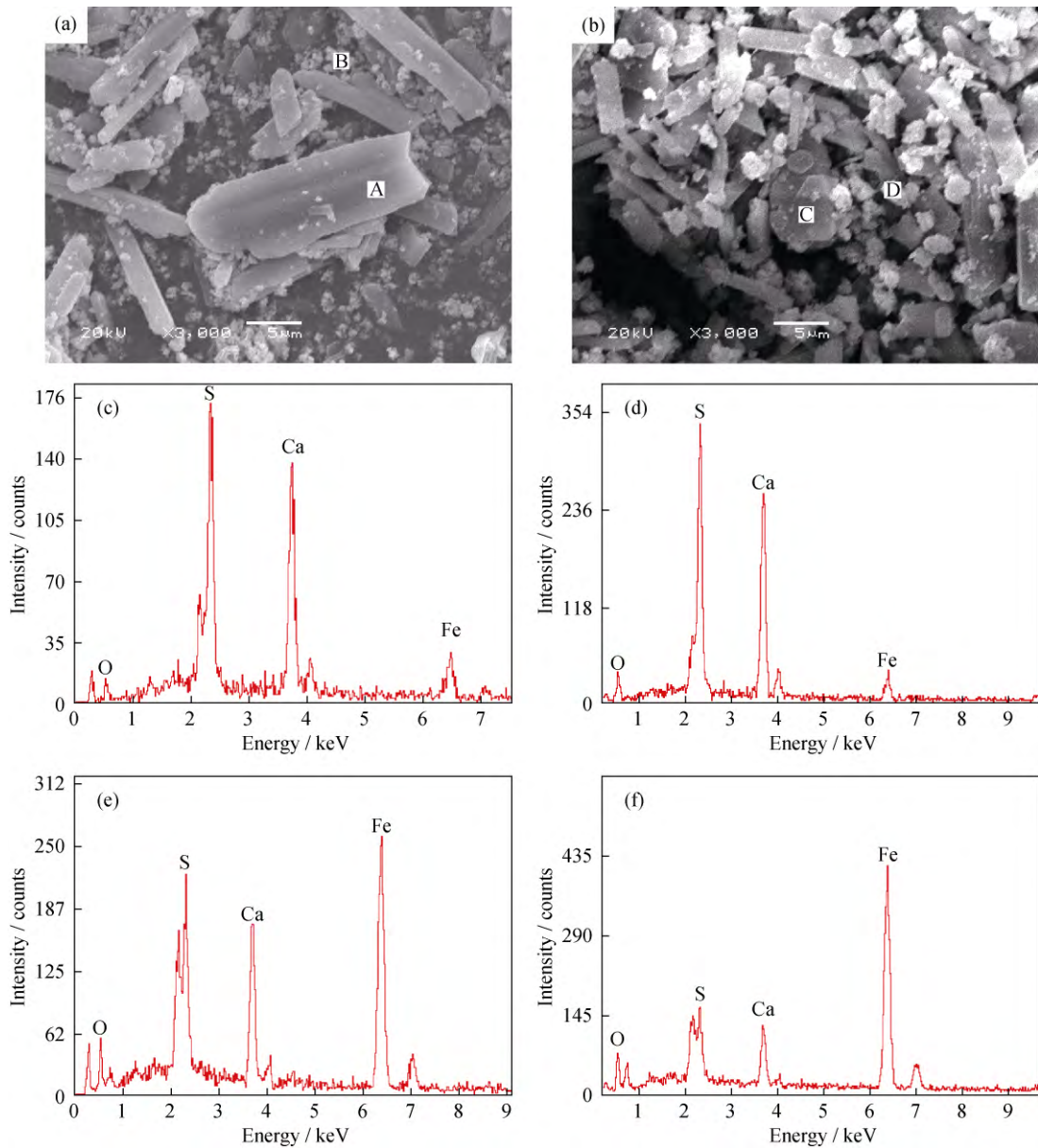


Fig. 5. SEM images of the mixed products without (a) and with (b) purification pretreatment and the corresponding EDS spectra of areas A (c), C (d), B (e), and D (f).

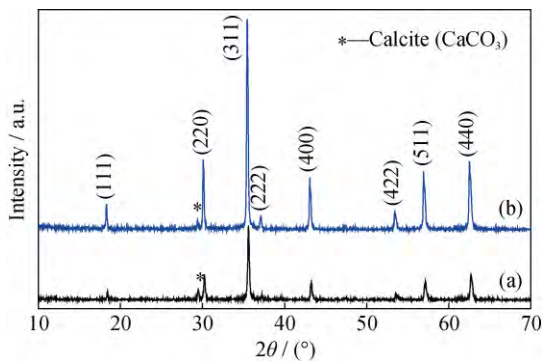


Fig. 6. XRD patterns of magnetite concentrates without (a) and with (b) purification pretreatment.

pretreatment, the magnetite was very tiny, indicating that the nucleation rate was much faster than the growth rate. However, the particle size increased when purification pretreatment was applied, suggesting that impurity reduction was likely to accelerate the nucleation and especially the growth rate. The particle size distribution of magnetite concentrates is shown in Fig. 8, which reveals that the particle size of magnetite concentrate obtained with the pretreatment was larger than that of the concentrate without the pretreatment; it also reveals that their median particle sizes were 2.35 and 1.55 μm , respectively. This finding is in good agreement with the SEM results in Fig. 7.

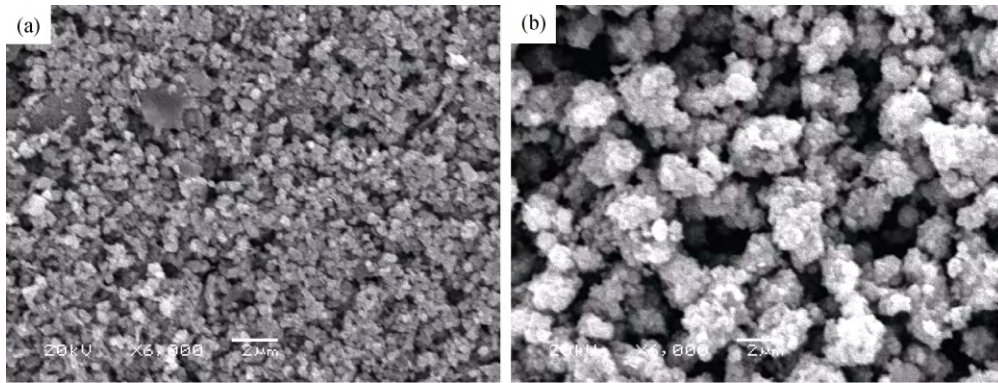


Fig. 7. SEM images of magnetite concentrates without (a) and with (b) purification pretreatment.

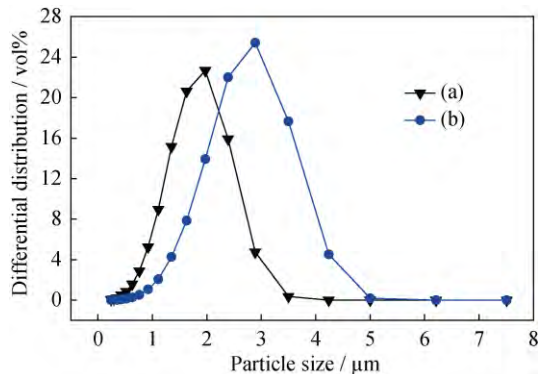


Fig. 8. Particle size distribution of magnetite concentrates without (a) and with (b) purification pretreatment.

The concentrations of impurities in magnetite concentrates without and with purification pretreatment were determined by ICP-OES; the results are shown in Table 4. As evident in Table 4, the concentrate obtained with purification pretreatment contained higher concentrations of Mg and Mn compared to the concentrate obtained without purification pretreatment, whereas the concentrate obtained with the pretreatment contained less Ca, S, Ti, Al, and Zn. Especially the concentration of Ti in magnetite concentrate obtained with purification pretreatment decreased from 1.59wt% to 0.004wt%. The results well accord with the previous results shown in Table 2 and Fig. 2. Thus, a higher-grade magnetite was obtained by purification pretreatment.

Table 4. Content of impurities in magnetite concentrates without and with purification pretreatment wt%

Experimental treatment	Ca	S	Mg	Ti	Mn	Al	Zn
Without pretreatment	2.91	1.05	0.20	1.59	0.45	0.09	0.03
With pretreatment	2.01	0.85	0.78	0.004	0.78	0.04	0.02

4. Conclusions

(1) Ferrous sulfate solution was purified by the addition

of NaOH solution to precipitate impurities. Under the optimal pH value of 3.5–4.0, the removal rates of Fe, Mg, Ti, Mn, Zn, and Al were 10.84%, 2.19%, 98.39%, 1.38%, 22.02%, and 52.72%, respectively.

(2) Magnetite was recovered from ferrous sulfate solution with calcium hydroxide as the precipitant. With purification pretreatment, the grade of iron in the magnetite concentrate was increased from 62.05% to 65.58%, while the recovery rate of iron decreased from 85.35% to 80.35%. The experimental results suggest that such purification pretreatment can reduce the conglutination between magnetite and gypsum, which facilitates subsequent magnetic separation of them. A higher grade magnetite with a greater crystallinity and with a larger particle size of 2.35 μm was obtained with purification pretreatment.

Acknowledgements

This research was financially supported by the Special Project on the Integration of Industry, Education and Research of Guangdong Province, China (No. 20013A090100013) and by the High Technology Research and Development Program of Xinjiang Uygur Autonomous Region of China (No. 201407300993).

References

- [1] P.H. Huang, B. Jiang, Z.Y. Zhang, X.L. Wang, X.D. Chen, X.S. Yang, and L. Yang, Recycling sulfur and iron resources in the waste ferrous sulfate, *J. Therm. Anal. Calorim.*, 119(2015), No. 3, p. 2229.
- [2] M.J. Gázquez, J.P. Bolívar, R. García-Tenorio, and F. Vaca, Physicochemical characterization of raw materials and co-products from the titanium dioxide industry, *J. Hazard. Mater.*, 166(2009), No. 2-3, p. 1429.
- [3] N. Guskos, G.J. Papadopoulos, V. Likodimos, S. Patapis, D. Yarmis, A. Przepiera, K. Przepiera, J. Majszczyk, J. Typek, M. Wabia, K. Aidinis, and Z. Drazek, Photoacoustic, EPR

- and electrical conductivity investigations of three synthetic mineral pigments: hematite, goethite and magnetite, *Mater. Res. Bull.*, 37(2002), No. 6, p. 1051.
- [4] Y.J. Zheng and Z.C. Liu, Preparation of monodispersed micaceous iron oxide pigment from pyrite cinders, *Powder Technol.*, 207(2011), No. 1-3, p. 335.
- [5] Y.J. Zheng and H. Teng, *Method for Preparing Iron Oxide Yellow from Fe³⁺ Solution*, Chinese Patent, Appl. 10200055.8, 2012.
- [6] Y.J. Zheng, Z.Q. Gong, B.Z. Chen, and L.H. Liu, Preparation of solid polyferric sulfate from pyrite cinders and its structure feature, *Trans. Nonferrous Met. Soc. China*, 13(2003), No. 3, p. 690.
- [7] N. Kanari, I. Filippova, F. Diot, J. Mochón, I. Ruiz-Bustanza, E. Allain, and J. Yvon, Utilization of a waste from titanium oxide industry for the synthesis of sodium ferrate by gas–solid reactions, *Thermochim. Acta*, 575(2014), p. 219.
- [8] L. Wu, Z.X. Wang, X.H. Li, H.J. Guo, L.J. Li, X.J. Wang, and J.C. Zheng, Cation-substituted LiFePO₄ prepared from the FeSO₄·7H₂O waste slag as a potential Li battery cathode material, *J. Alloys Compd.*, 497(2010), No. 1-2, p. 278.
- [9] E.L. Tavani and N.A. Lacour, Making of iron(III) tanning salts from a waste of the titanium recovery by the sulphate process, *Mater. Chem. Phys.*, 72(2001), No. 3, p. 380.
- [10] R. Lakshmanan and G. Kuttuva Rajarao, Effective water content reduction in sewage wastewater sludge using magnetic nanoparticles, *Bioresour. Technol.*, 153(2014), p. 333.
- [11] C. Jiang, R. Wang, and W. Ma, The effect of magnetic nanoparticles on *Microcystis aeruginosa* removal by a composite coagulant, *Colloids Surf. A*, 369(2010), No. 1-3, p. 260.
- [12] Y.R. Li, J. Wang, Y. Zhao, and Z.K. Luan, Research on magnetic seeding flocculation for arsenic removal by superconducting magnetic separation, *Sep. Purif. Technol.*, 73(2010), No. 2, p. 264.
- [13] GB/T 1863—2008, *Iron Oxide Pigments*, Standards Press of China, Beijing, 2008.
- [14] A. Biswal, B. Dash, B.C. Tripathy, T. Subbaiah, S.M. Shin, K. Sanjay, and B.K. Mishra, Influence of alternative alkali reagents on Fe removal during recovery of Mn as electrolytic manganese dioxide (EMD) from Mn sludge, *Hydrometallurgy*, 140(2013), p. 151.
- [15] J.A. Dean, *Lange's Handbook of Chemistry*, 15th Ed., Science Press, Beijing, 2003.
- [16] A. Šutka, S. Lagzdina, I. Juhnevica, D. Jakovlevs, and M. Maiorov, Precipitation synthesis of magnetite Fe₃O₄ nanoflakes, *Ceram. Int.*, 40(2014), No. 7, p. 11437.
- [17] L.Z. Shen, Y.S. Qiao, Y. Guo, and J.R. Tan, Preparation and formation mechanism of nano-iron oxide black pigment from blast furnace flue dust, *Ceram. Int.*, 39(2013), No. 1, p. 737.
- [18] L.Z. Shen, Y.S. Qiao, Y. Guo, and J.R. Tan, Preparation of nanometer-sized black iron oxide pigment by recycling of blast furnace flue dust, *J. Hazard. Mater.*, 177(2010), No. 1-3, p. 495.
- [19] X.C. Wei and R.C. Viadero Jr, Synthesis of magnetite nanoparticles with ferric iron recovered from acid mine drainage: Implications for environmental engineering, *Colloids Surf. A*, 294(2007), No. 1-3, p. 280.
- [20] R.Y. Hong, J.H. Li, H.Z. Li, J. Ding, Y. Zheng, and D.G. Wei, Synthesis of Fe₃O₄ nanoparticles without inert gas protection used as precursors of magnetic fluids, *J. Magn. Magn. Mater.*, 320(2008), No. 9, p. 1605.
- [21] T. Ishikawa, H. Nakazaki, A. Yasukawa, K. Kandori, and M. Seto, Influences of Co²⁺, Cu²⁺ and Cr³⁺ ions on the formation of magnetite, *Corros. Sci.*, 41(1999), No. 8, p. 1665.
- [22] Z.C. Liu and Y.J. Zheng, Effect of Fe(II) on the formation of iron oxide synthesized from pyrite cinders by hydrothermal process, *Powder Technol.*, 209(2011), No. 1-3, p. 119.